



## The influences of traces of oxygen and sulfide on the corrosion of copper in concentrated chloride solutions

S. Ramamurthy<sup>a</sup>, J. Chen<sup>b,\*</sup>, D. Zagidulin<sup>b</sup>, J.D. Henderson<sup>a</sup>, C. Lilja<sup>c</sup>, E. Bergendal<sup>c</sup>, M. Behazin<sup>d</sup>, N. Diomidis<sup>e</sup>, P.G. Keech<sup>d</sup>, J.J. Noël<sup>a,b</sup>, D.W. Shoesmith<sup>a,b</sup>

<sup>a</sup> Surface Science Western, London, Ontario N6G 0J3, Canada

<sup>b</sup> Department of Chemistry, University of Western Ontario, London, Ontario N6A 5B7, Canada

<sup>c</sup> Swedish Nuclear Fuel and Waste Management Company, SE-169 03 Solna, Sweden

<sup>d</sup> Nuclear Waste Management Organization, Toronto M4T 2S3, Canada

<sup>e</sup> National Cooperative for the Disposal of Radioactive Waste, Hardstrasse 73, Wetingen 5430, Switzerland

### ARTICLE INFO

#### Keywords:

- A. Copper
- B. XPS
- B. Raman spectroscopy
- C. Interfaces

### ABSTRACT

The corrosion of wrought, electrodeposited, and cold spray deposited copper was electrochemically monitored for ~160 days in 3 M NaCl solution containing traces of sulfide under anoxic and Ar-purged conditions. Corroded specimens were analyzed using scanning electron microscopy and Raman and X-ray photoelectron/Auger spectroscopies. Under anoxic conditions, corrosion was supported by sulfide only and the rate decreased with time causing only minor damage. Under low oxygen conditions maintained by Ar-purging, the rate increased with time and significant damage was observed, attributed to oxy-sulfur species formation. These results suggest that oxy-sulfur species, not just sulfide, are required to cause intergranular corrosion.

### 1. Introduction

The widely accepted approach for the safe management of used nuclear fuel is to dispose of it in a deep geological repository (DGR) in a stable geological formation [1,2]. The key engineered barriers are the used fuel container (UFC) and the surrounding bentonite clay which swells when wet to seal the DGR. In Canada, Sweden, and Finland, the chosen corrosion barrier will be Cu either as a shell over a cast iron insert (Sweden, Finland) or as a coating on carbon steel formed by electrodeposition and cold spray deposition [3].

Once the UFC is emplaced in a DGR, the specific corrosion processes that are possible will change as the exposure conditions evolve from initially warm, humid, and oxidizing to eventually cool, wet, and anoxic as the radioisotopes in the fuel decay, leading to a decrease in heat production. The O<sub>2</sub> trapped upon initial emplacement and sealing will be consumed by microbial and mineral reactions and minor corrosion of the container [3,4]. When the O<sub>2</sub> inventory is depleted, the dominant container degradation process will become a reaction with sulfide (SH<sup>-</sup>) generated remotely via the reaction of anaerobic sulfate-reducing bacteria (SRB) with sulfate (SO<sub>4</sub><sup>2-</sup>) in the groundwater and sealing materials [5,6].

Early predictions suggested oxic conditions could persist for decades [7,8], but more recent field studies indicate much shorter periods ranging from a few weeks to a few months [9]. While conservative estimates show that the extent of corrosion damage accumulated by the various oxic/anoxic corrosion processes [3] should not threaten the integrity of the UFC over the required lifetime, uncertainties remain over how corrosion will progress and what influences the early oxic period will exert on the long-term anoxic process. To resolve these uncertainties, studies under well-controlled redox conditions are essential, especially since SH<sup>-</sup> is well known to be unstable in the presence of dissolved O<sub>2</sub> [10–15] producing a multitude of potentially corrosive oxy-sulfur species.

This study compares long-term experiments (up to 160 days) on Cu specimens (wrought, electrodeposited, cold spray deposited) in aqueous concentrated chloride solutions under anoxic conditions (achieved in an anaerobic chamber) and under slightly oxidizing conditions (achieved by Ar sparging during laboratory bench-top experiments). The use of concentrated chloride solutions simulates the extremely saline groundwater encountered in the sedimentary host rock, a geosphere still under assessment as a possible location for a Canadian DGR [3]. In an attempt to emphasize the sensitivity of Cu corrosion to O<sub>2</sub> and SH<sup>-</sup>, experiments

\* Corresponding author.

E-mail address: [jchen496@uwo.ca](mailto:jchen496@uwo.ca) (J. Chen).

<https://doi.org/10.1016/j.corsci.2024.112047>

Received 16 February 2024; Received in revised form 5 April 2024; Accepted 8 April 2024

Available online 10 April 2024

0010-938X/© 2024 The Author(s). Published by Elsevier Ltd. This is an open access article under the CC BY license (<http://creativecommons.org/licenses/by/4.0/>).

were conducted with  $\leq$  micromolar  $[O_2]$  and  $[SH^-]$ . Such conditions are also relevant to a DGR when very low concentrations are anticipated [3].

## 2. Experimental

### 2.1. Materials

Cold sprayed specimens (Cu-CSA), annealed at 350°C for 1 hour under an Ar-purged atmosphere, were prepared and supplied by the National Research Council (NRC, Boucherville, Canada) [16]. The wrought Cu specimens (Cu-SKB) were O-free and P-doped (30–100 wt. ppm) and provided by the Swedish Nuclear Fuel and Waste Management Company (SKB, Solna, Sweden). Electrodeposited (Cu-ED) samples were supplied by Integran Technologies Inc. (Mississauga, Canada) using the procedure documented elsewhere [17]. Prior to each experiment, the specimen under study was ground successively with P1200- to P4000-grade SiC paper, washed in Type I H<sub>2</sub>O (resistivity  $\geq$  18.2 M $\Omega$ -cm), ultrasonically cleaned in methanol, washed with Type I H<sub>2</sub>O, and dried in a stream of Ar. Since no cathodic pretreatment was employed, the surfaces of Cu electrodes were covered with a thin air-formed oxide [18].

### 2.2. Solution

All experiments were conducted in a 3 M NaCl solution made up with NaCl (99.999% (metals basis)) supplied by Alfa Aesar using Type I H<sub>2</sub>O. To increase the salt purity on the cation basis by lowering the content of heavy metals (Pb, Hg, Sb, Cd, etc.), the supplier “purified” the NaCl salt using SH<sup>-</sup> to remove these heavy metals. As a consequence, the prepared NaCl solution contained some sulfide, but at levels  $\leq$  the analytical detection limit of  $\sim$ 1  $\mu$ M using a sulfide selective electrode.

### 2.3. Electrochemical procedures

Electrochemical measurements were performed in a three-electrode cell with the Cu specimen as the working electrode. A saturated calomel electrode (SCE) and a Pt foil were used as the reference and counter electrodes, respectively. The reference electrode was continuously immersed in the solution, and its potential change against another saturated calomel electrode (maintained in saturated KCl solution) was measured before and after the exposure test to be  $<$  5 mV. A Solartron 1480 Multistat or a Solartron 1287 potentiostat was used to measure and control potentials and record current responses. Corrware™/Corrview™ software (Scribner Associates) was used to control instrumentation and to record and analyze data. Corrosion potential ( $E_{CORR}$ ) and polarization resistance ( $R_p$ ) measurements were conducted periodically. The linear polarization resistance technique was conducted at a scan rate of 10 mV·min<sup>-1</sup> over the potential range  $E_{CORR} \pm$  5 mV (the corrosion rate is proportional to  $R_p^{-1}$ ).

Two sets of experiments were performed: (1) under Ar-purged conditions on the laboratory bench top, when small amounts of dissolved O<sub>2</sub> (estimated to be  $\leq$  1  $\mu$ M) would be expected in the electrochemical cell; and (2) in an Ar-purged anaerobic chamber (Canadian Vacuum Systems) maintained at a positive pressure (2–4 mbar) by an MBraun glove box control system (anoxic conditions). The O<sub>2</sub> concentration in the chamber was analyzed with an MBraun O<sub>2</sub> probe with a detection limit of 1.4 mg·m<sup>-3</sup>. In the anaerobic chamber, the minimum measurable  $[O_2]$  was set by the sensitivity of the O<sub>2</sub> sensor at 1 vppm, while the actual vapour phase (O<sub>2</sub> + H<sub>2</sub>O) concentration may have been considerably  $<$  1 vppm. Using Henry's Law, a value of 10<sup>-6</sup> atm (10<sup>-4</sup> kPa) for the partial pressure of O<sub>2</sub> in the chamber (the total pressure being 1.15 atm) and a Henry's Law constant of 769 L·atm·mol<sup>-1</sup> ( $7.79 \times 10^4$  L·kPa·mol<sup>-1</sup>) for O<sub>2</sub> at 298 K, the dissolved  $[O_2]$  in solution was estimated to be  $\leq$  1.3 nM [19,20]. In these exposure tests, the volume of the solution was 2 L, and the solution was stagnant and not replenished.

### 2.4. Characterization of specimens

Specimens were examined using optical microscopy and scanning electron microscopy, the latter with a Hitachi S-4500 field emission scanning electron microscope (SEM) equipped with an EDAX™ energy dispersive X-ray spectroscopy (EDS) system.

Raman spectroscopy was performed using a Renishaw 2000 Raman spectrometer equipped with a 632 nm He-Ne laser and an Olympus microscope. Spectra were obtained using a 50 $\times$  uncoated objective lens with the beam focused to a diameter of  $\sim$ 2  $\mu$ m. To minimize surface heating effects, the laser was used at 10 % of the full power. The spectrometer was calibrated against the 520.5 cm<sup>-1</sup> peak of Si.

X-ray photoelectron spectroscopy (XPS) analyses were performed with a Kratos AXIS Nova spectrometer using an Al K $\alpha$  monochromatic high energy ( $h\nu = 1486$  eV) source. The instrument work function was calibrated using the Au 4f<sub>7/2</sub> line with a binding energy = 83.96 eV for metallic Au. Survey scans were conducted over an area of 300  $\mu$ m by 700  $\mu$ m at a pass energy of 160 eV. High-resolution analyses were conducted over a similar analysis area at a pass energy of 20 eV. The Kratos charge neutralizer system was used on all specimens and the C 1s peak at 284.8 eV was used as a standard to correct for surface charging. High-resolution spectra were obtained for the Cu 2p and S 2p peaks and the Cu L<sub>3</sub>M<sub>4,5</sub>M<sub>4,5</sub> Auger peak and analyzed as described elsewhere [21].

## 3. Results

### 3.1. Corrosion measurements

Figs. 1 and 2 show the  $E_{CORR}$  and  $R_p$  values recorded under anoxic and Ar-purged conditions, respectively. Under anoxic conditions, Fig. 1,  $E_{CORR}$  for all three specimens quickly established steady-state values in the range  $-0.372$  V (vs. SCE) to  $-0.375$  V (vs. SCE) which were subsequently maintained for the duration of the exposure period. The  $R_p$  values for the individual specimens varied over the first  $\sim$ 30 days before adopting similar increasing values which tended towards steady-state at longer exposure times, with  $R_p$  for Cu-SKB approaching a value  $<$  2 times greater than those recorded for the other two specimens.

Under Ar-purged conditions, Fig. 2,  $E_{CORR}$  values for Cu-SKB and Cu-CSA again exhibit similar behaviour initially stabilizing around  $-0.385$  V (vs. SCE) before steadily increasing to values between  $-0.320$  V (vs. SCE) and  $-0.330$  V (vs. SCE) after  $\sim$ 110 days. In contrast to the increase observed under anoxic conditions,  $R_p$  values decreased steadily with exposure time from  $\sim$ 80 k $\Omega$ ·cm<sup>2</sup> to  $\sim$ 10–20 k $\Omega$ ·cm<sup>2</sup> indicating an increase in corrosion rate up to  $\sim$ 120 hours. Beyond 120 h of exposure to Ar-sparging ( $[O_2] \leq 1$   $\mu$ M),  $E_{CORR}$  for both Cu-SKB and Cu-CSA started to decrease and the corresponding  $R_p$  values initially increased slightly before diverging. It is uncertain why this occurred, but a possibility is that oxide formation became the dominant process once SH<sup>-</sup> was depleted. This could lead to opposing behaviours since the corrosion rate could be increased by the catalysis of O<sub>2</sub> reduction on Cu<sub>2</sub>S [22–26] but decreased by oxide formation. The sudden increase (by  $\sim$ 10 mV) in  $E_{CORR}$  after  $\sim$ 50 hours, which was accompanied by a slight decrease in  $R_p$ , could indicate a slight change in Ar-purging conditions leading to a small increase in the dissolved  $[O_2]$  and, hence, the corrosion rate. The absence of  $E_{CORR}/R_p$  values for Cu-ED under Ar-purged conditions was due to a loss of contact with the specimen after a few days of exposure. Although not shown, the  $E_{CORR}$  and  $R_p$  values recorded prior to this malfunction were similar in both value and trend to those shown in Fig. 2.

Table 1 compares the final  $E_{CORR}$  values recorded on Cu-SKB, Cu-ED and Cu-CSA to values measured in a similar experiment conducted under aerated conditions [2] indicating an increase in  $E_{CORR}$  as the  $[O_2]$  increases. The slightly higher values recorded under Ar-purged conditions compared to those recorded under anoxic conditions indicate the persistence of slightly oxidizing conditions in the former case. Fig. 3

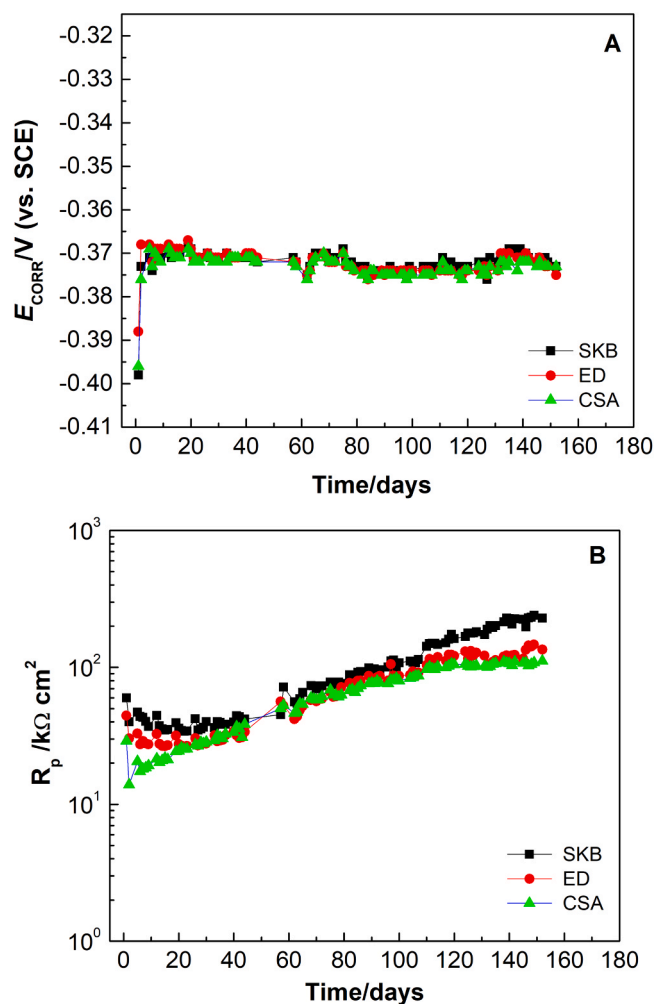


**Fig. 1.** Corrosion potential ( $E_{CORR}$ ) (A) and polarization resistance ( $R_p$ ) values (B) measured on Cu-SKB, Cu-ED, and Cu-CSA in a 3 M NaCl solution (contaminated with  $\text{SH}^-$ ) under anoxic conditions (in an anaerobic chamber:  $[\text{O}_2] \leq 1.3$  nM) [2].

summarizes the  $R_p$  values recorded over the exposure period of 20–150 days showing a decrease in corrosion rate under anoxic conditions but an increase under Ar-purged conditions. The  $R_p$  values recorded under aerated conditions are strongly influenced by the build-up of an atacamite ( $\text{Cu}_2(\text{OH})_3\text{Cl}$ ) deposit and have been discussed previously [2].

### 3.2. Characterization of corrosion products

Fig. 4 shows scanning electron micrographs of the specimen surfaces after exposure under anoxic conditions. For the Cu-SKB and Cu-ED specimens, slight general corrosion was observed with the original polishing lines induced during specimen preparation remaining visible. For the Cu-CSA specimen, slightly more surface damage was observed. In all cases, a scattered surface deposit of fine particulates was formed. Although not a particularly surface-sensitive analytical technique, EDX analyses show the particles have a higher S content ( $\sim 2$  wt%) compared to the general surface ( $\sim 0.2$  wt%). This observation is consistent with expectations for Cu corrosion in dilute anoxic chloride solutions containing low  $[\text{SH}^-]$  [27] in which aggregates of chalcocite ( $\text{Cu}_2\text{S}$ ) particulates were shown to form on Cu-SKB [27] by the generation of Cu-transporting sulfide complexes ( $\text{Cu}(\text{SH})_2^-$ ) and  $\text{Cu}_3\text{S}_3$  clusters [28].

Fig. 5 shows that the extent of corrosion damage was significantly greater on Cu-CSA and Cu-SKB under Ar-purged conditions than under

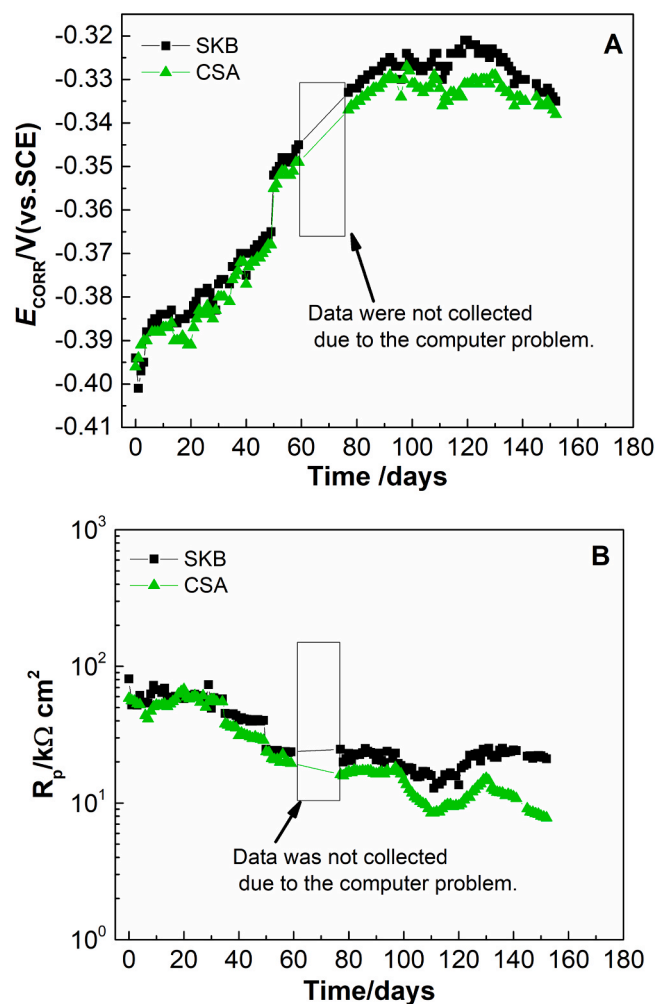


**Fig. 2.** Corrosion potential ( $E_{CORR}$ ) (A) and polarization resistance ( $R_p$ ) values (B) measured on Cu-SKB and Cu-CSA in a 3 M NaCl solution (contaminated with  $\text{SH}^-$ ) under Ar-purged conditions ( $[\text{O}_2] \leq 1$   $\mu\text{M}$ ).

**Table 1**

Corrosion potential ( $E_{CORR}$ ) values recorded on Cu-SKB, Cu-ED, and Cu-CSA after 60 or 160 days of exposure to 3 M NaCl solution.

Anaerobic chamber (160 days)	Ar-purged (160 days)	$\text{O}_2$ -purged (60 days) [2]
-0.372 V to -0.375 V	-0.330 V to -0.340 V	-0.170 V to -0.250 V*

\* The wide range in aerated solutions depends on the morphology of the Cu(II) deposit present on the surface (Standish et al. [2])

anoxic conditions. The morphology of the damage to the Cu-CSA specimen was a consequence of the smearing effect of the preparatory polishing process, with the labeled site (marked as "1") indicating the location from which a cold spray particle was dislodged during specimen preparation. As observed on specimens exposed under anoxic conditions, a fine particulate deposit was observed on the Cu-SKB specimen.

Fig. 6 (A and B) shows Raman spectra recorded on Cu-CSA after exposure to anoxic conditions and Cu-SKB after exposure to Ar-purged conditions. These spectra were representative of spectra recorded on all specimens under both exposure conditions. The grounds for assigning individual peaks to  $\text{Cu}_2\text{O}$  and  $\text{Cu}_2\text{S}$  have been discussed elsewhere [29–34]. In both cases, the presence of  $\text{Cu}_2\text{O}$  and  $\text{Cu}_2\text{S}$  was confirmed. Under anoxic conditions (when the dissolved  $[\text{O}_2] \leq 1.3$  nM), this suggested the air-formed oxide present on the Cu surface upon immersion in the solution was not completely converted to  $\text{Cu}_2\text{S}$  [34]. The higher  $\text{Cu}_2\text{S}/\text{Cu}_2\text{O}$  signal intensity ratio for Region 1 compared to Region 2,

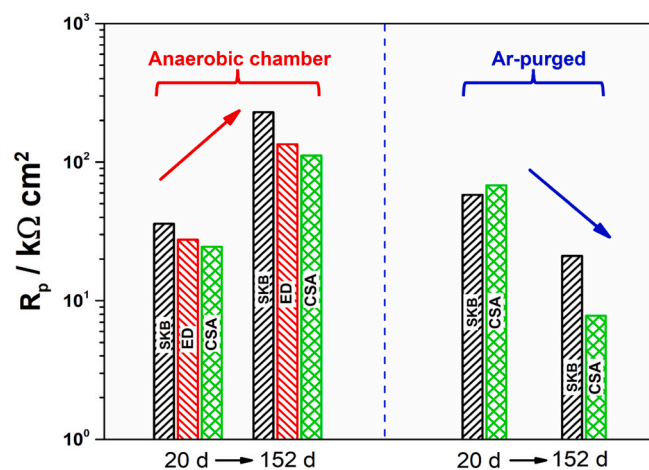


Fig. 3. Polarization resistance ( $R_p$ ) values measured after 20 and 152 days of exposure to a 3 M NaCl solution (contaminated with  $\text{SH}^-$ ) under anaerobic chamber (anoxic) and Ar-purged conditions.

Fig. 6A, could reflect the presence of nanoparticulate  $\text{Cu}_2\text{S}$  deposits within the analyzed area. Under Ar-purged conditions, Fig. 6B, the lower  $\text{Cu}_2\text{S}/\text{Cu}_2\text{O}$  ratio generally observed could indicate the joint formation of oxide and sulfide when a small continuous supply of dissolved  $\text{O}_2$  was available.

Fig. 7 shows high-resolution XPS and Auger spectra recorded on Cu-CSA after exposure to an anoxic environment. Similar spectra were obtained on other specimens. The Cu  $2p_{3/2}$  peak, Fig. 7A, could contain contributions from Cu(0), Cu(I) and Cu(II) states, which are in some cases inseparable, but the absence of a shake-up satellite peak in region A indicates the absence of Cu(II) states. This was confirmed by the Cu  $L_{3M_{4,5}M_{4,5}}$  Auger spectrum, Fig. 7B, which showed no contribution from Cu(II) and indicated the surface was mainly covered by a thin  $\text{Cu}_2\text{S}$  layer. The Cu  $2p_{3/2}$  and Cu  $L_{3M_{4,5}M_{4,5}}$  spectra recorded after an Ar-purged experiment, Fig. 8, showed minor differences to those recorded under anoxic conditions. The apparent domination of  $\text{Cu}_2\text{S}$  over  $\text{Cu}_2\text{O}$  may suggest an outer layer of sulfide on a partially converted  $\text{Cu}_2\text{O}$  layer.

Fig. 9A and B show the S  $2p_{3/2}$  and S  $2p_{1/2}$  peaks for anoxic (A) and Ar-purged (B) exposure conditions. Since the dissolved  $[\text{O}_2]$  under anoxic conditions was insignificant, the sulfite ( $\text{SO}_3^{2-}$ ) and sulfate ( $\text{SO}_4^{2-}$ ) peaks indicate some degree of atmospheric oxidation occurred on the surface during the transfer of the specimen from the electrochemical cell to the vacuum chamber of the spectrometer. Whether this was due to the oxidation of residual traces of  $\text{SH}^-$  remains unresolved. The absence of Cu(II) states under such conditions confirmed significant oxidation was avoided. As shown in Fig. 9B for Ar-purged conditions, the intensity for the peak attributed to one oxy-sulfur species (i.e.,  $\text{SO}_4^{2-}$ ) is significantly more prominent. Comparison of these spectra for a number of areas on a range of specimens (i.e., Cu-SKB, Cu-ED and Cu-CSA) showed that this difference was consistently observed indicating the possibility of the formation of oxy-sulfur species under Ar-purged conditions when the  $[\text{O}_2]$  throughout the exposure period was small but significant.

#### 4. Discussion

Under anoxic conditions, the decrease in corrosion rate over the duration of the experiment unaccompanied by a change in  $E_{\text{CORR}}$  indicated a transport-controlled corrosion process in the solution as observed previously in  $\text{SH}^-$  solutions containing  $5 \times 10^{-5} \text{M}$   $\text{SH}^-$  [5,27,35,36]. Since the  $[\text{O}_2]$  was negligible, the only available oxidant was the  $\text{SH}^-$  present as an impurity in the concentrated  $\text{Cl}^-$  solution. The corrosion of Cu at low  $[\text{SH}^-]$  was expected to be transport controlled [5,27,36], leading to  $\text{Cu}_2\text{S}$  formation (as observed in this study) with the

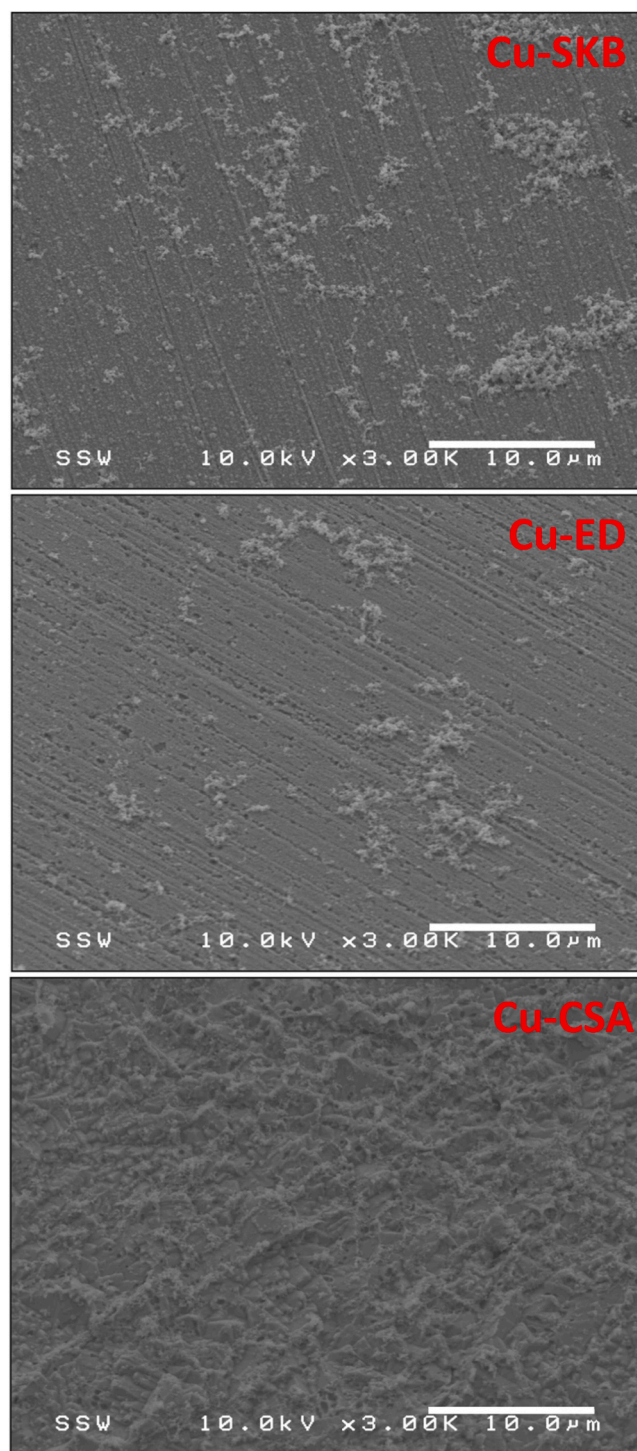


Fig. 4. SEM images of Cu-SKB, Cu-ED, and Cu-CSA surfaces after exposure for 168 days to a 3 M NaCl solution (contaminated with  $\text{SH}^-$ ) under anaerobic chamber (anoxic) conditions.

rate falling as the limited amount of  $\text{SH}^-$  was consumed and its flux to the Cu surface decreased [37]. At the low and uncertain  $[\text{SH}^-]$  used in this study, the Raman analyses showed that, on many areas of the surface, the  $\text{Cu}_2\text{O}$  film present upon immersion was not totally converted to  $\text{Cu}_2\text{S}$ . The observation of a thin scattered deposit of  $\text{Cu}_2\text{S}$  was consistent with previous observations that corrosion in solutions containing low  $[\text{SH}^-]$  ( $5 \times 10^{-5} \text{M}$ ) [6] leads to the formation of nanoparticulate aggregated deposits formed by the combined transport and deposition of  $\text{Cu}(\text{SH})_2^-$  complexes and  $\text{Cu}_3\text{S}_3$  clusters.

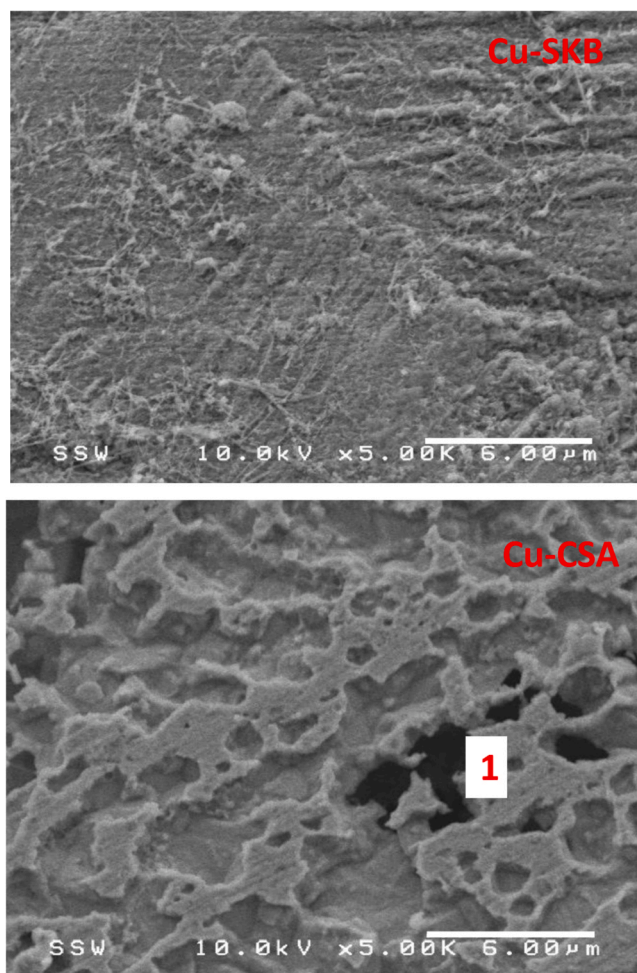
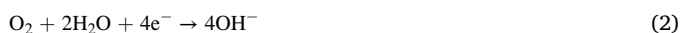
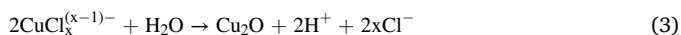


Fig. 5. SEM images of Cu-SKB and Cu-CSA surfaces after exposure for 166 days to a 3 M NaCl solution (contaminated with  $\text{SH}^-$ ) under Ar-purged conditions. Location 1 on the Cu-CSA surface shows a location from which a cold spray particle was dislodged during the surface polishing process prior to the experiment.

When a small  $[\text{O}_2]$  was present in the Ar-purged experiment, the initial rates were similar to those observed in the absence of  $\text{O}_2$  but increased with time leading to clear visual damage to the Cu surface. Since the  $[\text{O}_2]$  would have been maintained approximately constant by the persistent, but not totally efficient, Ar-purging, this increase in rate could not be attributed to the direct corrosion of Cu due to  $\text{O}_2$  reduction, a process which in  $\text{Cl}^-$  solution is well known to proceed via the production of Cu-Cl complexes [38]



which could lead to the formation of  $\text{Cu}_2\text{O}$  via hydrolysis.



The homogeneous oxidation of Cu(I) to Cu(II)



is also possible [39]. If this reaction occurred, it was to an extent that did not lead to the formation of  $\text{Cu}^{2+}$  deposits (such as atacamite ( $\text{Cu}_2(\text{OH})_3\text{Cl}$ )) on the Cu surface since no Cu(II) states were observed in surface analyses by either Raman spectroscopy or XPS/Auger spectroscopy. Alternatively, the reaction of the Cu(I)-Cl complex with  $\text{SH}^-$  could lead to  $\text{Cu}_2\text{S}$  formation [6,40],

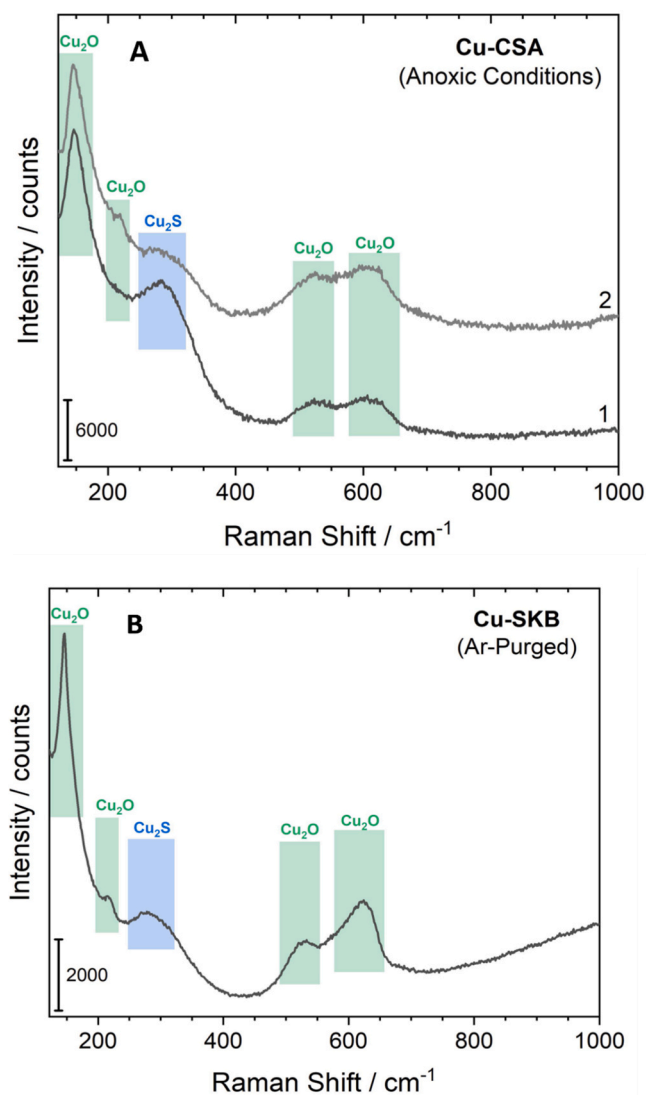
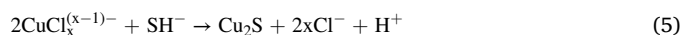


Fig. 6. Raman spectra recorded on (A) a Cu-CSA surface after 168 days exposure to a 3 M NaCl solution (contaminated with  $\text{SH}^-$ ) under anoxic conditions, and on (B) a Cu-SKB surface exposed to a 3 M NaCl solution (contaminated with  $\text{SH}^-$ ) for 166 days under Ar-purged conditions.



a reaction that cannot be ruled out in the present study, since  $\text{Cu}_2\text{S}$  was detected on the Cu surface by both Raman spectroscopy and XPS/Auger spectroscopy.

Whether reactions (4) and (5) occurred to any significant extent was uncertain given the low  $[\text{SH}^-]$  and  $[\text{O}_2]$  present, but their occurrence would not offer an explanation for why the corrosion rate increased with time in Ar-purged solution. On the contrary, their occurrence would be expected to, at best, maintain the rate (at constant  $[\text{O}_2]$ ) or decrease it (as  $\text{SH}^-$  was depleted).

In the presence of dissolved  $\text{O}_2$ ,  $\text{SH}^-$  is well known to undergo oxidation [10–15]. Early studies showed that oxidation in neutral solutions similar to those used in this study [10,11] led to a mixture of sulfate ( $\text{SO}_4^{2-}$ ), sulfite ( $\text{SO}_3^{2-}$ ), and thiosulfate ( $\text{S}_2\text{O}_3^{2-}$ ) the first two of which were observed as surface species by XPS in this study. The overall reaction was shown to be first order with respect to both  $\text{SH}^-$  and  $\text{O}_2$ , with  $\text{S}_2\text{O}_3^{2-}$  the dominant product when the  $[\text{O}_2]/[\text{SH}^-]$  ratio was low [15,41], and  $\text{SO}_4^{2-}$  the main product when this ratio was high [10,15].

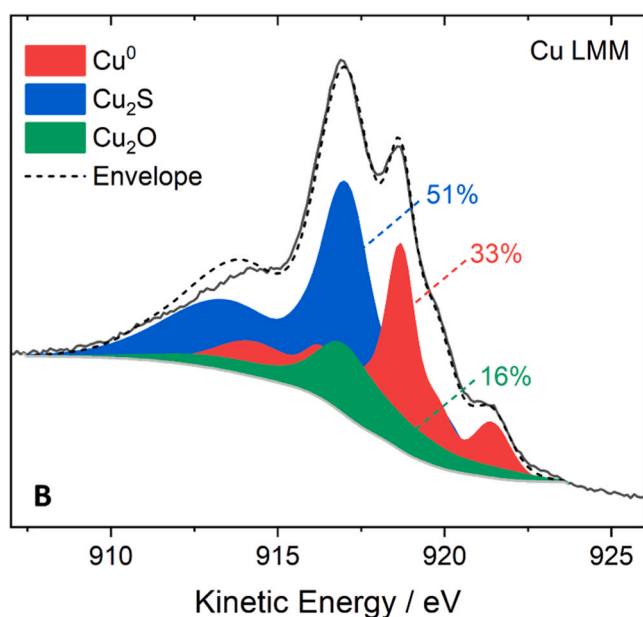
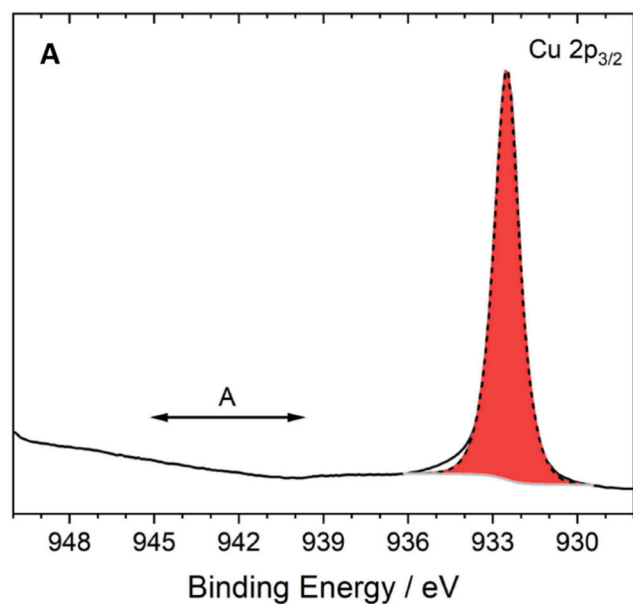


**Fig. 7.** (A) XPS and (B) Auger spectra recorded on a Cu-CSA surface after exposure for 168 days to a 3 M NaCl solution (contaminated with  $\text{SH}^-$ ) under anoxic conditions. Region A on the XPS spectrum indicates the binding energy range within which a satellite peak indicating the presence of Cu(II) would be observed.

Since  $\text{SO}_4^{2-}$  is the most stable species in the presence of  $\text{O}_2$ , the increase in the exposure time of  $\text{SH}^-$  solution to  $\text{O}_2$  (e.g., 70 h [10]) yields  $\text{SO}_4^{2-}$  as the main oxidation product [10,15], consistent with the XPS results. In the present Ar-purged experiments, in which the  $[\text{O}_2]$  was maintained constant while  $[\text{SH}^-]$  steadily decreased,  $\text{S}_2\text{O}_3^{2-}$  would be expected to be the dominant oxy-sulfur species formed initially when the  $[\text{SH}^-]$  was at its highest, and the  $[\text{O}_2]/[\text{SH}^-]$  ratio at its lowest.

Once formed,  $\text{S}_2\text{O}_3^{2-}$  is relatively stable to disproportionation [15]



and, hence, more readily available to act as an oxidant for Cu.

At low  $[\text{SH}^-]$  (10–100  $\mu\text{M}$ ), the overall oxidation mechanism has been suggested [15,42] as

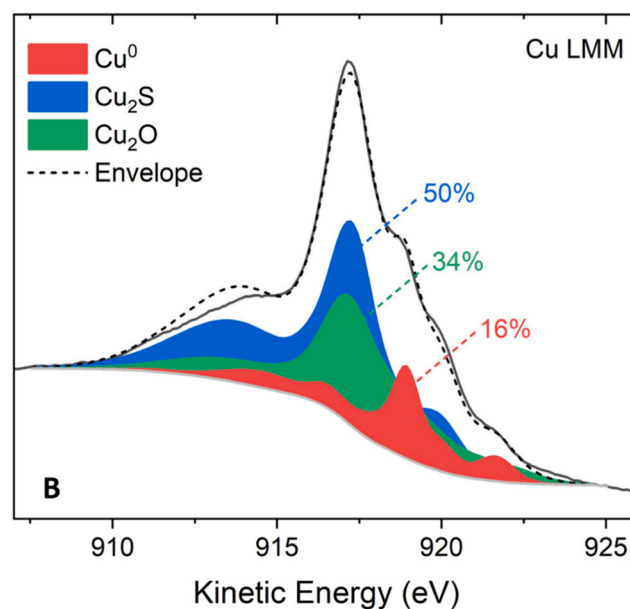
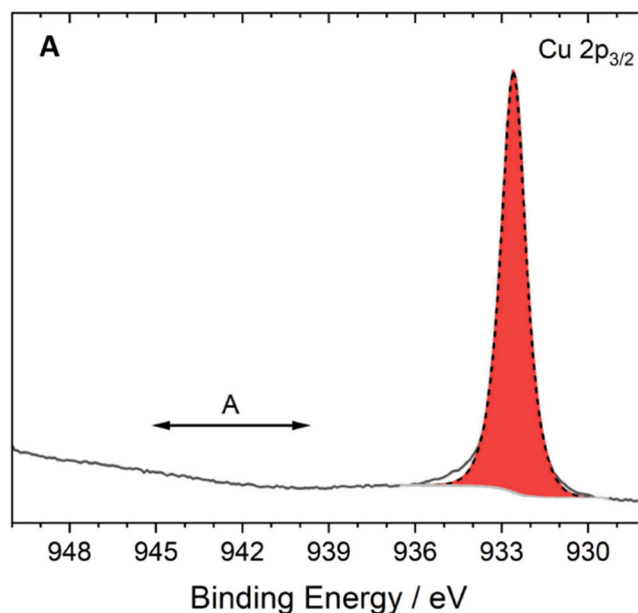


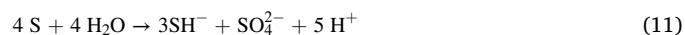
**Fig. 8.** (A) XPS and (B) Auger spectra recorded on a Cu-SKB surface after exposure for 166 days to a 3 M NaCl solution (contaminated with  $\text{SH}^-$ ) under Ar-purged conditions. Region A on the XPS spectrum indicates the binding energy region within which a satellite peak indicating the presence of Cu(II) would be observed.



$\text{S}_2\text{O}_3^{2-}$  is a metastable anion which can be both oxidized and reduced or can disproportionate [43]. Its reduction, which is thought to proceed via elemental S



can lead via disproportionation to the formation of  $\text{SH}^-$



and further corrosion of Cu leading to  $\text{Cu}_2\text{S}$  formation [1,6,27,28]

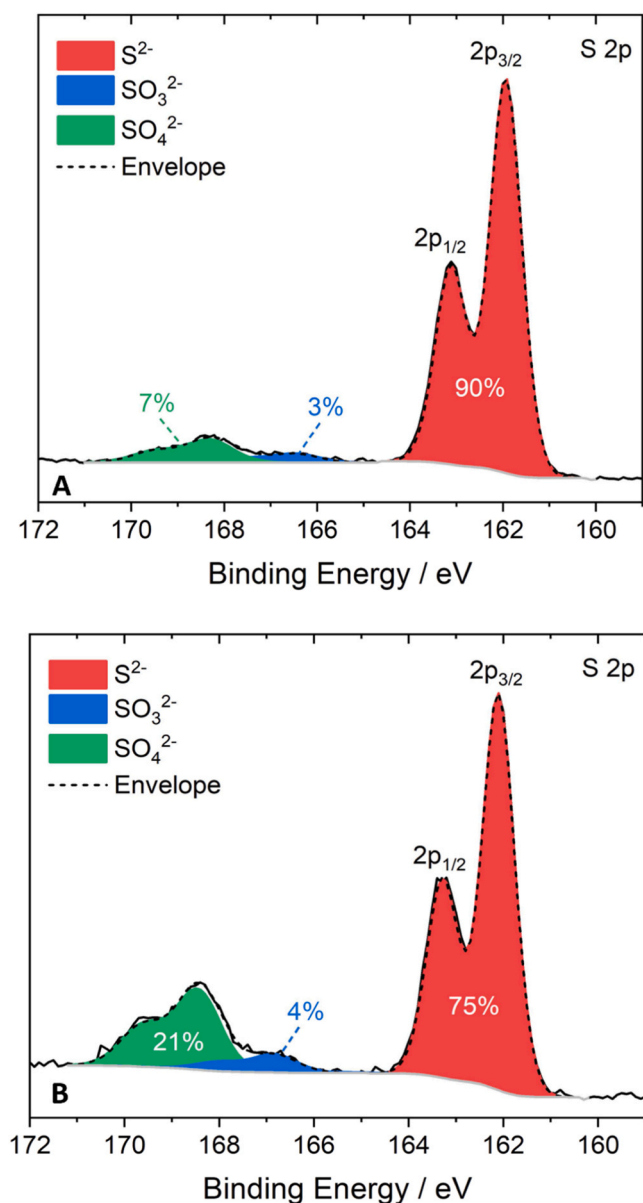


Fig. 9. Sulfur XPS spectra recorded on (A) a Cu-CSA surface after exposure for 168 days to a 3 M NaCl solution (contaminated with  $\text{SH}^-$ ) under anoxic conditions; and (B) a Cu-CSA surface after exposure for 166 days to a 3 M NaCl solution (contaminated with  $\text{SH}^-$ ) under Ar-purged conditions.



consistent with Raman spectroscopic analyses in this study. Since Cu corrosion yielding  $\text{Cu}_2\text{S}$  formation could have occurred directly due to the presence of  $\text{SH}^-$  in the original solution, this route via  $\text{S}_2\text{O}_3^{2-}$  offers a secondary mechanistic route for corrosion leading to  $\text{Cu}_2\text{S}$  and would offer a possible explanation for the observed increased corrosion in Ar-purged solutions when very low  $[\text{O}_2]$  was present. Additionally, the forced convection from Ar-purging could have accelerated the rate at short exposure times but not at longer times when  $\text{SH}^-$  became depleted. The rate of the reaction sequence (10) to (12) could be high since  $\text{SH}^-$  can be completely sequestered by Cu (as  $\text{Cu}_2\text{S}$  or  $\text{Cu}_3\text{S}_3$  [6]). This would make the detection of the intermediate  $\text{S}_2\text{O}_3^{2-}$  difficult. Such difficulties were reported when the oxidation rate of  $\text{SH}^-$  was accelerated in the presence of  $\text{Fe}^{2+}$  and  $\text{Mn}^{2+}$  [44,45]. Since the formation of  $\text{S}_2\text{O}_3^{2-}$  by the oxidation of  $\text{SH}^-$  in  $\text{O}_2$ -containing solutions is accelerated by the presence of micromolar  $[\text{Cu}^{2+}]$  [46], any  $\text{Cu}^{2+}$  formed via reaction (4) would have contributed to the increase in corrosion rate observed in

inefficiently Ar-purged solution. While  $\text{Cl}^-$  would be involved in the corrosion process (reactions (1) to (5)), Zhang and Millero [15] showed in studies in seawater and chloride-free  $\text{H}_2\text{O}$  that  $\text{Cl}^-$  exerted no significant influence on the homogeneous oxidation of  $\text{SH}^-$  to oxy-sulfur species.

$\text{S}_2\text{O}_3^{2-}$  is known as a very aggressive anion which can cause corrosion damage to a variety of materials, mainly passive alloys such as stainless steel and Ni alloys [43]. This combination of  $\text{SH}^-$  oxidation to  $\text{S}_2\text{O}_3^{2-}$  (reactions (7) and (9)) coupled with its reduction in support of Cu corrosion (reactions (10) and (11)) could act as an accelerating reaction cycle promoting the corrosion of Cu until the supply of  $\text{SH}^-$  was exhausted. Such an accelerating reaction cycle would be promoted within locations (e.g., pores in corrosion products, grain boundary) within which dilution of oxy-sulfur species (e.g.,  $\text{S}_2\text{O}_3^{2-}$ ) via transport to the bulk solution would be limited. When Cu and its alloys were exposed to aerated  $\text{SH}^-$  solutions [22–26, 47] or  $\text{S}_2\text{O}_3^{2-}$  solutions [48,49], their surfaces were covered with porous and defective oxide/sulfide mixtures and their corrosion rates were accelerated. Intergranular corrosion (IGC) of Cu and its alloys was also observed in aerated 3.5 wt% NaCl solutions containing  $\text{SH}^-$  [50–52].

While the results described in this study do not show IGC, they demonstrate that a combination of  $\text{SH}^-$  and dissolved  $\text{O}_2$ , even at micromolar levels achievable with extensive Ar purging, leads to the acceleration of Cu corrosion and the observation of oxy-sulfur species on the corroding Cu surface.

## 5. Summary and conclusions

Under anoxic conditions ( $[\text{O}_2] \leq 1.3 \text{ nM}$ ), corrosion led to the formation of scattered deposits of  $\text{Cu}_2\text{S}$  and also the partial conversion of the native  $\text{Cu}_2\text{O}$  present on the Cu specimen surface upon immersion. The corrosion rate decreased with time as  $\text{SH}^-$ , the only available oxidant, was consumed, and only minimal corrosion damage was observed.

Under Ar-purged conditions ( $[\text{O}_2] \leq 1 \text{ }\mu\text{M}$ ), a similar  $\text{Cu}_2\text{O}/\text{Cu}_2\text{S}$  layer and scattered deposits of  $\text{Cu}_2\text{S}$  were formed, but the corrosion rate increased with time and the corrosion damage was observable by SEM. This increase was attributed to the formation of oxy-sulfur species by the reaction of  $\text{SH}^-$  with the available  $\text{O}_2$ .

The nature of the Cu (Cu-SKB, Cu-ED, Cu-CSA) had no significant influence on the corrosion rates under either anoxic or Ar-purged conditions.

Although IGC was not observed at the low  $[\text{O}_2]$  and  $[\text{SH}^-]$  used in our experiments, the increased corrosion rate when oxy-sulfur species were formed emphasizes the need to avoid even low  $[\text{O}_2]$  when investigating such a process.

## Author Statement

All the listed authors have contributed to this paper and agree that we submit it for review by the journal Corrosion Science. We confirm that the experimental results and calculations are authentic and that the manuscript is original, unpublished, and not being considered for publication elsewhere.

## Conflict of interest

The authors have stated explicitly that there are no conflicts of interest in connection with this article.

## CRediT authorship contribution statement

**S. Ramamurthy:** Writing – original draft, Methodology, Investigation, Formal analysis, Data curation, Conceptualization. **J. Chen:** Writing – review & editing, Writing – original draft, Methodology, Investigation, Formal analysis, Data curation, Conceptualization. **D.**

**Zagidulin:** Methodology, Investigation. **J.D. Henderson†:** Formal analysis, Data curation. **C. Lilja:** Writing – review & editing, Project administration, Funding acquisition. **E. Bergendal:** Writing – review & editing, Funding acquisition. **M. Behazin:** Writing – review & editing, Project administration, Funding acquisition. **N. Diomidis:** Writing – review & editing, Funding acquisition. **P. Keech:** Writing – review & editing, Funding acquisition. **J.J. Noel:** Writing – review & editing, Supervision, Methodology. **D. Shoesmith:** Writing – review & editing, Writing – original draft, Supervision, Methodology.

### Declaration of competing interest

The authors declare that they have no known competing financial interests or personal relationships that could have appeared to influence the work reported in this paper.

### Data Availability

Data will be made available on request.

### Acknowledgments

This research was jointly funded by the Nuclear Waste Management Organization (Toronto, Canada) and by Nagra (Wettingen, Switzerland). Rebecca Sarazen, Mark Beisinger, and Jonas Hedberg from Surface Science Western (London, Canada) are acknowledged for assistance in processing SEM/EDX, XPS/Auger, and Raman spectroscopic data.

### References

- [1] D.S. Hall, P.G. Keech, An overview of the Canadian corrosion program for the long-term management of nuclear waste, *Corros. Eng. Sci. Technol.* 52 (sup1) (2017) 2–5.
- [2] T. Standish, J. Chen, R. Jacklin, P. Jakupi, S. Ramamurthy, D. Zagidulin, P. G. Keech, D.W. Shoesmith, Corrosion of copper-coated steel high level nuclear waste containers under permanent disposal conditions, *Electrochim. Acta* 211 (2016) 331–342.
- [3] D.S. Hall, M. Behazin, W.J. Binns, P.G. Keech, An evaluation of corrosion processes affecting copper-coated nuclear waste containers in a deep geological repository, *Prog. Mater. Sci.* 118 (2021) 100766.
- [4] F. King, D.S. Hall, P.G. Keech, Nature of the near-field environment in a deep geological repository and the implications for the corrosion behaviour of the containers, *Corros. Eng. Sci. Technol.* 52 (sup 1) (2017) 25–30.
- [5] F. King, J. Chen, Z. Qin, D.W. Shoesmith, C. Lilja, Sulphide transport control of the corrosion of copper canisters, *Corros. Eng. Sci. Technol.* 52 (sup 1) (2017) 210–216.
- [6] J. Chen, Z. Qin, T. Martino, M. Guo, D.W. Shoesmith, Copper transport and sulphide sequestration during copper corrosion in anaerobic aqueous sulphide solutions, *Corros. Sci.* 131 (2018) 245–251.
- [7] F. King, M. Kolar, A numerical model for the corrosion of copper nuclear fuel containers, *Mater. Res. Soc. Symp. Proc.* 412 (1996) 555–562.
- [8] P. Wersin, K. Spahiu and J. Bruno, Time evolution of dissolved oxygen and redox conditions in a HLW repository, Swedish Nuclear Fuel and Waste Management Company Report, 1994, SKB-TR-406-02.
- [9] H.R. Müller, B. Garitte, T. Vogt, S. Köhler, T. Sakaku, H. Weber, T. Spillman, M. Hertrich, J.K. Becker, N. Giroud, V. Cloet, N. Diomidis, T. Vieto, Implementation of the full-scale emplacement (FE) experiment at the Mont Terri rock laboratory, *Swiss J. Geosci.* 110 (2017) 287–306.
- [10] J.D. Cline, F.A. Richards, Oxygenation of hydrogen sulfide in seawater of constant salinity, temperature and pH, *Environ. Sci. Technol.* 3 (1969) 838–840.
- [11] K.Y. Chen, J.C. Morris, Kinetics of oxidation of aqueous sulfide by O<sub>2</sub>, *Environ. Sci. Technol.* 6 (1972) 529–537.
- [12] D.J. O'Brian, F.G. Birkner, Kinetics of oxygenation of reduced sulfur species in aqueous solution, *Environ. Sci. Technol.* 11 (1977) 1114–1120.
- [13] F.J. Millero, The thermodynamics and kinetics of the hydrogen sulfide system in natural waters, *Mar. Chem.* 18 (1986) 121–147.
- [14] F.J. Millero, S. Hubinger, M. Fernandez, S. Garnett, Oxidation of H<sub>2</sub>S in seawater as a function of temperature, pH and ionic strength, *Environ. Sci. Technol.* 211 (1987) 439–443.
- [15] J.A. Zhang, F.J. Millero, The products from the oxidation of H<sub>2</sub>S in seawater, *Geochim. Cosmochim. Acta* 57 (1993) 1705–1718.
- [16] P. Vo, D. Poirier, J.-G. Legoux, P.G. Keech, Application of copper coatings onto used fuel canisters for the Canadian nuclear industry, in: J. Karthikeyan, C. Kay (Eds.), *High Pressure Cold Spray: Principles and Applications*, ASM International, 2016, pp. 253–276.
- [17] P.G. Keech, P. Lin, N. Mahalanobis, Electrodeposited copper coatings for used fuel containers. In: 35th Annual CNS Conference Proceedings, Canadian Nuclear Society, Saint John, Canada, 2015.
- [18] M. Guo, J. Chen, T. Martino, C. Lilja, J.A. Johansson, M. Behazin, W.J. Binns, P. G. Keech, J.J. Noël, D.W. Shoesmith, The nature of the copper sulfide film grown on copper in aqueous sulfide and chloride solutions, *Mater. Corros.* 72 (1-2) (2021) 300–307.
- [19] R. Sander, Compilation of Henry's law constants (version 4.0) for water as solvent, *Atmos. Chem. Phys.* 15 (2015) 4399–4981.
- [20] R. Partovi-Nia, S. Ramamurthy, D. Zagidulin, J. Chen, R. Jacklin, P.G. Keech, D. W. Shoesmith, Corrosion of a cold spray deposited copper coating on steel substrates, *Corrosion* 71 (2015) 1237–1247.
- [21] M.C. Biesinger, Advanced analysis of copper X-ray photoelectron spectra, *Surf. Interface Anal.* 49 (2017) 1325–1334.
- [22] B.C. Syrett, Accelerated corrosion of copper in flowing pure water contaminated with oxygen and sulfide, *Corrosion* 33 (7) (1977) 257–262.
- [23] J.P. Gudas, H.P. Hack, Parametric evaluation of susceptibility of Cu-Ni alloys to sulfide induced corrosion in sea water, *Corrosion* 35 (6) (1979) 259–264.
- [24] B.C. Syrett, The mechanism of accelerated corrosion of copper-nickel alloys in sulphide-polluted seawater, *Corros. Sci.* 21 (1981) 187–209.
- [25] L.E. Eiselstein, B.C. Syrett, S.S. Wing, R.D. Caligiuri, The accelerated corrosion of Cu-Ni alloys in sulphide-polluted seawater: mechanism no. 2, *Corros. Sci.* 23 (1983) 223–239.
- [26] S.J. Yuan, S.O. Pehkonen, Surface characterization and corrosion behavior of 70/30 Cu-Ni alloy in pristine and sulfide-containing simulated seawater, *Corros. Sci.* 49 (3) (2007) 1276–1304.
- [27] J. Chen, Z. Qin, D.W. Shoesmith, Long-term corrosion of copper in a dilute anaerobic sulfide solution, *Electrochim. Acta* 56 (2011) 7854–7861.
- [28] J. Chen, Z. Qin, T. Martino, D.W. Shoesmith, Non-uniform film growth and micro/macro galvanic corrosion of copper in aqueous sulfide solutions containing chloride, *Corros. Sci.* 114 (2017) 72–78.
- [29] J.M. Smith, Z. Qin, F. King, L. Werme, D.W. Shoesmith, Sulfide film formation on copper under electrochemical conditions, *Corrosion* 63 (2007) 135–144.
- [30] G. Niaux, Surface-enhanced Raman spectroscopic observations of two kinds of adsorbed OH<sup>-</sup> ions at a copper electrode, *Electrochim. Acta* 45 (2000) 3507–3519.
- [31] M. Liu, J. Li, In-situ characterization of initial corrosion behaviour of copper in neutral 3.5% (wt.) NaCl solution, *Materials* 12 (2019) 2164.
- [32] A. Kudelski, Structures of monolayers formed from different HS-(CH<sub>2</sub>)<sub>2</sub>-X thiols on gold, silver and copper: comparative studies by surface-enhanced Raman scattering, *J. Raman Spectrosc.* 34 (2003) 853–862.
- [33] J.R. Mycroft, G.M. Bancroft, N.S. McIntyre, J.W. Lorimer, I.R. Hill, Detection of sulphur and polysulphides on electrochemically oxidized pyrite surfaces by X-ray photoelectron spectroscopy and Raman spectroscopy, *J. Electroanal. Chem.* 292 (1990) 139–152.
- [34] E.S. Alaei, M. Guo, J. Chen, M. Behazin, E. Bergendal, C. Lilja, D.W. Shoesmith, J. J. Noël, The transition from used fuel container corrosion under oxidic conditions to corrosion in an anoxic environment, *Mater. Corros.* 74 (2023) 1690–1706.
- [35] J. Chen, Z. Qin, D.W. Shoesmith, Kinetics of corrosion film growth on copper in neutral chloride solutions containing small concentrations of sulfide, *J. Electrochem. Soc.* 157 (2010) C338–C345.
- [36] J. Chen, Z. Qin, D.W. Shoesmith, Key parameters determining structure and properties of sulphide films formed on copper corroding in anoxic sulphide solutions, *Corros. Eng. Sci. Technol.* 49 (2014) 415–419.
- [37] J. Chen, Z. Qin, D.W. Shoesmith, Copper corrosion in aqueous sulfide solutions under nuclear waste disposal conditions, *Mat. Res. Soc. Symp. Proc.* 1475 (2012) 465–470.
- [38] C. Deslouis, B. Tribollet, G. Mengoli, M.M. Musiani, Electrochemical behaviour of copper in neutral aerated chloride solution. I – Steady-state investigation, *J. Appl. Electrochem.* 18 (1988) 373–383.
- [39] V.K. Sharma, F.J. Millero, The oxidation of Cu(I) in electrolyte solutions, *J. Solut. Chem.* 17 (1988) 581–599.
- [40] M. Guo, J. Chen, T. Martino, M. Biesinger, J.J. Noël, D.W. Shoesmith, The susceptibility of copper to pitting corrosion in borate-buffered aqueous solutions containing chloride and sulfide, *J. Electrochem. Soc.* 166 (2019) C550–C558.
- [41] B.A. Skopintsev, A.V. Karpov, O.A. Vershinina, Study of the dynamics of some sulfur compounds in the Black Sea under experimental conditions, *Sov. Oceanogr.* 4 (1959) 55–72.
- [42] M. Avrahami, R.M. Golding, The oxidation of the sulphide ion at very low concentrations in aqueous solutions, *J. Chem. Soc. A* (1968) 647–651.
- [43] L. Choudhary, D.D. Macdonald, A. Alfantazi, Role of thiosulfate in the corrosion of steels: A review, *Corrosion* 71 (2015) 1147–1168.
- [44] G.W. Luther III, T.M. Church, D. Powell, Sulfur speciation and sulfide oxidation in the water column of the Black Sea, *Deep-Sea Res. A: Oceanogr. Res. Pap.* 38 (1991) S1121–S1137.
- [45] F.J. Millero, The oxidation of H<sub>2</sub>S in Black Sea waters, *Deep-Sea Res. A: Oceanogr. Res. Pap.* 38 (1991) S1139–S1150.
- [46] G.F. Vazquez, J.-F. Zhang, F.J. Millero, Effect of transition metals on the rate of oxidation of H<sub>2</sub>S in seawater, *Geophys. Res. Lett.* 16 (1989) 1363–1366.
- [47] K. Rahmouni, M. Keddad, A. Shiri, H. Takenouti, Corrosion of copper in 3 % NaCl solution polluted by sulfide ions, *Corros. Sci.* 47 (2005) 3249–3266.
- [48] H.M. Ezuber, Effect of temperature and thiosulfate on the corrosion behaviour of 90-10 copper nickel alloys in seawater, *Anti-Corros. Methods Mater.* 56 (2009) 168–172.
- [49] A.R. Al Rashed, F.M. Kharafi, B.G. Ateya, L.M. Ghayad, Effect of thiosulfate ions on the corrosion behaviour of copper in simulated seawater, *Egypt J. Chem.* 57 (2014) 109–127.

- [50] F.M. Al Kharafi, I.M. Ghayed, B.G. Ateya, Rapid intergranular corrosion of Cu in sulfide-polluted salt water, *Electrochem. Solid State Lett.* 11 (2008) G15–G18.
- [51] F.M. Al Kharafi, I.M. Ghayed, B.G. Ateya, Sulfide induced intergranular corrosion of copper in salt water containing benzotriazole, *e-J. Surf. Sci. Nanotechnol.* 9 (2011) 306–310.
- [52] X. Zhu, T. Lei, Characteristics and formation of corrosion product films of 70Cu–30Ni alloy in seawater, *Corros. Sci.* 44 (1) (2002) 67–79.